"This is a preprint of an article published in Loheide, S. P., II (2008) A method for estimating subdaily evapotranspiration of shallow groundwater using diurnal water table fluctuations. Ecohydrology., 1, p. 59-66, DOI: 10.1002/eco.7"

The final version is available from the Ecohydrology journal homepage at:
http://www3.interscience.wiley.com/

A method for estimating subdaily evapotranspiration of shallow groundwater using diurnal water table fluctuations

Steven P. Loheide II
University of Wisconsin – Madison
Department of Civil and Environmental Engineering
1415 Engineering Dr
Madison, WI 53706
loheide@wisc.edu

Abstract:

Diurnal water table fluctuations are a common feature of well hydrographs recorded in wetlands, riparian areas, and similar environments where shallow groundwater supports phreatophytic vegetation. Historically, this periodic signal has been used to estimate daily groundwater consumption by this vegetation and has shown that this is typically a very large component of the water budget. As interest in ecohydrology grows and the need for finer resolution estimates of groundwater consumption increases, new, cost-effective measurement methodologies must be developed. Here, a method is proposed that uses the observed rate of water table decline during the day to estimate phreatophytic groundwater consumption while using the nighttime records to account for other groundwater fluxes to/from the vicinity of the well at all times. Variably-saturated groundwater flow modeling was used to create a synthetic data set to test the methodology, and results showed that accurate, subdaily (15 minute) estimates of phreatophytic groundwater consumption were obtained. The method was also applied to a pre-existing data set to demonstrate the usefulness of the technique.

Keywords: Evapotranspiration, Ecohydrology, Groundwater, Variably-saturated, Numerical modeling, Water table, Phreatophyte, Riparian

Introduction:

Water table fluctuations have long been recognized as a valuable source of information for inferring daily groundwater consumption (ET_G) by phreatophytic vegetation, where ET_G is the portion of total ET that comes from groundwater [e.g., White, 1932; Troxell, 1936; Gatewood et al., 1950; Meyboom, 1967]. In groundwater dependent ecosystems water table fluctations appear to be nearly ubiquitous [ie Bleby et al, 1997; Loheide et al., 2005; Engel et al., 2005; Butler et al., 2007; Lautz, 2007]. The diurnal ET signal has also been observed in streams [Bond et al., 2002; Czikowsky and Fitzjarrald, 2004]; although, other factors such as snowmelt [Lundquist and Cayan, 2002] and streambed temperature [Constantz, 1998] can also cause diurnal patterns in streamflow. With growing interest in the ecohydrology of groundwater-dependent ecosystems, [Eamus and Froend, 2006], researchers are searching for cost-effective methods for measuring ET_G not only at daily intervals, but also as it varies throughout the day.

Recently, Schilling [2007] and Schilling and Kiniry [2007] have suggested daily water table fluctuations may contain information on ET_G rates at a time scale finer than daily resolution. Schilling [2007] and Schilling and Kiniry [2007] use the time rate of change of the water table to quantify the removal of groundwater by vegetation, however they do not generalize the method to account for the groundwater flux toward the riparian zone. This flux of groundwater replenishes the water removed by phreatophytic vegetation. While this flux of groundwater occurs continuously, it can be identified by the recovery of the water table during the night and is common to most published watertable fluctuations [White, 1932; Troxell, 1936; Gatewood et al., 1950; Meyboom,

67 1967; Bleby et al, 1997; Loheide et al., 2005; Engel et al., 2005; Butler et al., 2007;
68 Lautz, 2007.] The purposes of this article are to 1) formalize a general methodology for
69 estimating ET_G at short (15-minute) time scales, 2) validate the method using a synthetic
70 data set, and 3) apply the method to field data to demonstrate its utility.
71
72 **Theory:**
73 As first introduced in the classic work of White [1932], diurnal water table
74 fluctuations, such as those depicted in Figure 1, are generated by vegetation that extracts
75 groundwater during the daylight hours only. As a result, the water table typically falls
76 from shortly after sunrise until sunset, the period during which solar energy is available
77 to drive evapotranspiration. After sunset, the transpiration rate of vegetation drops nearly
78 to zero. When this occurs, the water table begins to rise as water is flowing toward the
79 vicinity of the well to replace the water that has been extracted through the process of
80 ET_G. While the water table records show this recovery only at night, water is, in fact,
81 flowing, both day and night, toward regions where vegetation is extracting groundwater.
82 As a consequence, if not for this recovery caused by groundwater flow toward regions
83 from which it is being extracted, the observed ET_G induced drop in the water table would
84 be even greater than observed during the daylight hours.
85 The time rate of change of groundwater storage in the vicinity of the well is equal
86 to the time rate of change in water table depth (*dWT/dt*) times the readily available
87 specific yield, S_y^* [-], where the * indicates the important difference between the
88 classically defined specific yield and the readily available specific yield associated with
89 short time scales and a shallow watertable [Meyboom, 1967; Nachabe, 2002; Loheide et

al., 2005]. As proposed by White (1932) and shown in Eq (1), this change in storage is controlled by the net flow of groundwater to/from the vicinity of the well, *r(t)* [L/T], and the evapotranspirative groundwater consumption rate, ET_G [L/T]:

$$S_y^* \frac{dWT}{dt} = r(t) - ET_G(t) \qquad \text{... eq (1)}$$

Fluxes are defined as positive toward the vicinity of the well and water table depth is defined as zero at the land surface and becomes increasingly negative as the water table becomes deeper. At times when ET_G is zero, Equation 1 simplifies to:

$$S_y^* \frac{dWT}{dt} = r(t) \qquad \text{... eq (2)}$$

White [1932], originally assumed that this rate was constant and Loheide et al. [2005] demonstrated that this assumption produced reasonable results for the White method because a representative recovery rate could be determined from the nighttime record. However, as first noted by Troxell [1936] and evidenced by the curvature of the recovery periods in Figure 1, the recovery rate is not constant over time. As a result, the recovery rate must be estimated as a function of time. During times of zero ET_G, this can readily be calculated as the recovery slope times the readily available specific yield. This recovery is driven by water flowing from areas of higher hydraulic head to replenish the water removed through the process of ET_G during the day. If one assumes this source of recovery water maintains a constant head, a function relating the inflow rate to the head difference between the water table at the observation location and the head at the nearby recovery source could be obtained. In this case, since the head at the recovery source is constant, this relationship would only be a function of the water table position at the

111 observation location. This relationship could be estimated from the observed water table
112 record during times of zero ET_G as:

113 $$r(WT) = S_y^* \frac{dWT}{dt} \qquad \text{... eq (3)}$$

114 Because of nonlinearities associated with unsaturated flow processes in the vadose zone,
115 three-dimensional groundwater flow patterns, and transient effects, a mathematical form
116 for this relationship cannot be specified for the general case. In practice, this function
117 could be obtained from the observed water table records obtained from midnight to 6 am,
118 (a period in which ET_G is assumed to be zero), and can be assumed linear over a short
119 time period and a small range in water table elevation.

120 However, it is not necessarily the case that the head at the recovery source
121 remains constant; rather, I suggest that it is more likely that it changes with a long-term
122 trend similar to that observed at the water table. A clear field example of this case is
123 shown in figure 6 of Butler et. al (2007) with three wells within a phreatophyte
124 dominated riparian zone showing clear diurnal fluctuations and one well outside the
125 riparian zone showing no fluctuations but following a similar declining trend to all other
126 well records. The main difference is that the diurnal oscillations observed near the water
127 table are muted or nonexistent at the recovery source as sketched in the inset graph of
128 Figure 1. For this analysis, it is assumed that the rate of change of head at the recovery
129 source is equal to the overall rate of water table change at the observation location. The
130 overall trend of the water table record can be found through a linear regression of the
131 period of analysis, which results in a trend slope (m_T) and intercept (b_T). The period of
132 analysis in this study included the recovery periods before and after the day for which

133 ET_G is being calculated. The detrended water table depth (WT_{DT}) is obtained by
134 subtracting this trend from a portion of the observed water table record as follows:

135 $$WT_{DT}(t) = WT(t) - m_T * t - b_T \qquad \text{... eq (4)}$$

136 With these assumptions, the detrended hydraulic head of the recovery source (H_{DT}) is a
137 constant. After applying this detrending procedure for the period of analysis, a
138 relationship can be determined to predict dWT_{DT}/dt as a function of the detrended water
139 table depth, $\Gamma(WT_{DT})$, using periods of zero ET_G. I propose using the detrended
140 observations between midnight and 6 am on the morning of and on the morning after the
141 day of interest to determine $\Gamma(WT_{DT})$. If the assumption is valid that the overall trend of
142 the observed water table is equal to the trend of the hydraulic head of the recovery
143 source, then the function $\Gamma(WT_{DT})$, defined in Eq (5) from periods of zero ET_G, should be
144 very similar for consecutive nights.

145 $$\Gamma(WT_{DT}) = \left[\frac{dWT_{DT}}{dt}\right] \qquad \text{... eq (5)}$$

146 For the purpose of this analysis, it is assumed that this function is approximately linear
147 over the small range of a diurnal water table fluctuation. A best-fit estimate of the
148 function $\Gamma(WT_{DT})$ is found using the detrended observations between midnight and 6 am
149 on the morning of and on the morning after the day of interest. Then the net inflow rate
150 can be estimated for the period of analysis using:

151 $$r(t) = S_y^*\left[\Gamma(WT_{DT}(t)) + m_T\right] \qquad \text{... eq (6)}$$

152 Once $r(t)$ is estimated in this fashion, ET_G is calculated directly through rearrangement of
153 Eq (1):

154 $$ET_G(t) = r(t) - S_y^* \frac{dWT}{dt} \qquad \text{... eq (7)}$$

155

156 **Methodology testing using simulated water table fluctuations:**

157 Using an approach similar to that of Loheide et al., [2005], numerical, variably-
158 saturated, groundwater flow modeling was employed to create a synthetic data set to test
159 the reliability of the proposed method for extracting subdaily groundwater
160 evapotranspiration signals from diurnal water table fluctuations. Comsol Multiphysics, a
161 general-purpose finite element modeling environment that has recently found application
162 in both saturated (i.e. [Cardenas and Wilson, 2007]) and variably-saturated (i.e. [Loheide
163 and Gorelick, 2007]) groundwater flow modeling was chosen to perform this simulation.
164 The flow domain investigated, shown in Figure 2, consists of a phreatophyte-dominated
165 floodplain and an upland region, and is typical of many riparian environments. Two-
166 dimensional, variably-saturated, transient groundwater flow modeling was performed
167 using Richards' Equation as shown below:

168 $$\left[C(\psi)+\left(\frac{\theta-\theta_R}{\theta_S-\theta_R}\right)(\rho_f g)\left(x_p(1-\theta_R)+x_f\theta_R\right)\right]\frac{\partial\psi}{\partial t}=\nabla\left(K\ (\psi)\nabla(\psi+z)\right)+\mathrm{Q_s} \qquad \text{... eq (8)}$$

169 where θ is the water content (-), θ_R is the residual water content (-), θ_S is the water
170 content at saturation (-), ψ is the pressure head (L), K(ψ) is the unsaturated hydraulic
171 conductivity (L/T), $C(\psi)=\delta\theta/\delta\psi$ (1/L), ρ_f is the density of the fluid (M/L^3), g is the
172 gravitational constant (L/T^2), x_f is the compressibility of the fluid (1/P), x_p is the
173 compressibility of the solid (1/P), and Q_s is a source/sink term (1/T). To describe the soil
174 moisture characteristic curves, the functional forms given by van Genuchten [1980] were
175 used and are shown below:

$$\theta = \theta_R + \frac{\theta_S - \theta_R}{\left[1 + (\alpha|\psi|)^n\right]^m} \quad \text{... eq (9)}$$

176

$$K(\theta) = K_S \left\{ \frac{\theta - \theta_R}{\theta_S - \theta_R} \right\}^{1/2} \left\{ 1 - \left[\left(\frac{\theta - \theta_R}{\theta_S - \theta_R} \right)^{1/m} \right]^m \right\}^2 \quad \text{... eq (10)}$$

177 where K_S is the saturated hydraulic conductivity (L/T), and α (1/L), n (-), and m (-) are
178 empirical coefficients with $m=1-1/n$. Hydraulic property values typical of a loamy soil
179 were used in the simulations: K= 4 x 10^{-6} m/s, α=1.5 m^{-1}, n=2 , θ_s=0.45 ; and θ_r=0.08 .
180 The aquifer compressibility was 1x10^{-6} Pa^{-1}.

181 All domain boundaries are treated as no flow boundaries and recharge and stream-
182 aquifer interactions are not considered, similar to the Case B of Loheide et al., [2005]
183 where a riparian area with a dry streambed is considered. The root water extraction zone
184 is 50 cm thick and the top is located at a depth of 30 cm beneath the floodplain. Neither
185 surface evaporation nor water extraction from the upper 30 cm of the soil zone is
186 considered. The initial condition used in the simulation is represented by a horizontal
187 water table at a position 10 cm below the elevation of the floodplain with hydrostatic
188 conditions in the underlying aquifer and the overlying vadose zone.

189 Water table fluctuations were simulated by imposing 9 days of *ET* cycling on and
190 off, which is represented in the model by a time-dependent, groundwater sink uniformly
191 distributed in the root uptake zone. During this period a square-wave pattern of ET_G was
192 simulated for the first six days, followed by a triangular pattern, a double-peaked pattern,
193 and another square-wave pattern. The purpose in changing the ET_G forcing function was
194 to create a variety of water table responses, which follow a spin-up period of 5 days.
195 During this simulation, a mesh consisting of ~46,000 elements, with spacing of ~0.01m

196 in the vicinity of the observation location was used, and time steps never exceeded 300
197 seconds. The water table position was found by interpolating for the z-position where
198 ψ=0 at each time step. The final synthetic data set was then created by sub-sampling this
199 time series to one with a 15-minute sampling frequency and adding a small random error
200 to each measurement. The patterns and rate of groundwater extraction and the resulting
201 water table fluctuations are shown in Figure 3.

202 The data for three days of this record associated with an ET_G forcing in the
203 square-wave, triangular, and double-peaked patterns were analyzed and will be referred
204 to as days 5, 6, and 7, respectively. All steps of this process for day 5 are shown in
205 Figure 4. First, a subset of data, from 8pm the previous night to 8am the next day, was
206 selected for each day of interest in order to include the recovery periods both proceeding
207 and following the ET_G induced drawdown of interest as shown in Figure 4a. For
208 visualization purposes, this data was shifted vertically so that the y-axis plotted near zero,
209 the detrended data could be plotted on the same axis, and the differences in slopes could
210 be seen. Secondly, the time rate of change of water table position (*dWT/dt*) was
211 calculated every 15 minutes using the slope estimated from the data at the time of the
212 estimate and the data points 15 minutes before and after this time. As shown in Figure
213 4b, this slope is positive during the nighttime hours, negative during daylight hours, and
214 changes systematically with the absolute value of the slope decreasing through both
215 nighttime and daylight periods. In Figure 4c, *dWT/dt* for the two recovery periods are
216 plotted against depth to the water table. Both of these relationships are linear; however,
217 there is a significant offset between these relationships. In Figure 4a, we have detrended
218 the plot of water table position, and the slope of this detrended water table record

(dWT_{DT}/dt) is plotted against detrended water table depth in Figure 4d. The best fit line in Figure 4d represents $\Gamma(WT_{DT})$. It is important to note that for both the night preceding and following the day of interest, the relationships $\Gamma(WT_{DT})$ collapse to define a single relationship. This detrending procedure is the key to this analysis because it allows estimation of the recovery rate (i.e. Eq 6) for any detrended water table depth, including those occurring during periods of ET_G. Finally, ET_G for this period is estimated using equations 6 and 7 with a readily available specific yield value of 0.055. This value is between the values of S_y^* predicted by Loheide et al [2005] for a silt loam (0.037) and a loam (0.075). This estimate, which is plotted in Figure 4e, reasonably estimates the ET_G rate specified in the simulation, with a root mean square error of 0.061 mm/hr.

The estimated ET_G rates using this method are shown not only for this square-wave ET_G pattern, but also for the triangular and double-peaked input patterns in Figure 5. All three patterns were reproduced using synthetic water table records and the method proposed here. The root mean square error for the square-wave, triangular, and double-peaked ET_G cases are 0.061, 0.038, and 0.038 mm/hr, respectively. While this level of error may be acceptable for many applications, there are several systematic biases that should be noted. For the square-wave case, where there is a step change in the ET_G rate, there is significant error immediately after ET_G begins or ends. The cause of this extreme error is that the change in the root uptake rate results in an abrupt change in the hydraulic gradient supplying water to the root uptake zone both from the vadose zone above and from deeper groundwater. This abrupt change in hydraulic gradient causes the position of the watertable (the location where Ψ=0) to respond abruptly, but the soil moisture profile above does not respond as fast. Because of this time lag and transient changes in the

242 shape of the soil moisture profile, the change in water table position is much greater than
243 would be predicted using the specific yield. Thus, ET_G is greatly over predicted near the
244 flow reversal associated with the modeled step change in ET_G. In natural environments,
245 the change in ET_G will never be this abrupt. In the triangular case, a related, but less
246 severe, bias exists. As ET_G is increasing in the model, the proposed predictive
247 methodology consistently overestimates ET_G, whereas the opposite is true when ET_G is
248 decreasing. As the rate of water table decline accelerates, the soil moisture profile
249 becomes less steep, resulting in a smaller readily available specific yield and an
250 overprediction of ET_G. The opposite occurs as the rate at which the water table falls
251 decreases. The same phenomenon can be seen in the ET_G estimates resulting from the
252 double-peaked pattern simulation.
253
254 **Example Application**
255 The utility of this approach will be demonstrated using a pre-existing data set that
256 was collected in a well screened across the water table in a riparian meadow located in
257 the Last Chance Watershed in Plumas National Forest, CA. Detailed site descriptions
258 can be found in Loheide and Gorelick [2005, 2006, and 2007]. The water table
259 fluctuations collected at this well are shown in Figure 6a for a two week period at the
260 beginning of August. These diel fluctuations typically have a magnitude of ~4 cm and
261 are very regular on all days except August 8, which was the only day with significant
262 cloud cover.
263 ET_G for this record was calculated using the method proposed here. A readily
264 available specific yield in the range of 0.06-0.08 was assumed, resulting in the range of

265 ET_G estimates plotted in Figure 6b. For comparison, potential *ET* was calculated on a 15
266 minute interval for a hypothetical reference crop with an assumed crop height of 0.12 m
267 and a fixed surface resistance of 70 s m-1. This standardized reference crop is consistent
268 with the sedges growing at the site. The reference ET was calculated using air
269 temperature, wind speed, soil temperature, solar radiation and humidity data from a
270 weather station located ~2m from the well for this period using standard methods
271 described by Allen et al., [1998]. It is evident that the pattern of estimated ET_G and the
272 potential *ET* are very similar; the ET_G estimates show that the vegetation is typically
273 transpiring at a rate just under the potential rate. On August 8, both ET_G and the potential
274 *ET* are significantly less than all other days due to the cloud cover; however, the potential
275 and actual patterns of *ET* on this day differ. This may indicate that the stomata remain
276 partially closed during the early portion when conditions are not optimal for the
277 vegetation; thus the vegetation is transpiring at a rate less than the potential *ET*. In figure
278 7, potential ET has been plotted against estimated ET_G using a S_y^*=0.08. Since the plot is
279 comparing potential ET with the groundwater component of actual ET, a 1:1 relationship
280 is not expected; however a correlation between these parameters is demonstrated. This
281 plot shows that ET_G is consistently less than potential ET. The negative ET_G estimates
282 are the result of pressure transducer noise and misfit between actual slope of the
283 detrended water table, dWT_{DT}/dt and the function $\Gamma(WT_{DT})$, which is used to predict this
284 slope based on detrended water table depth.
285
286
287

Discussion

The method proposed here has been shown to provide reasonable estimates of the rate of phreatophytic groundwater consumption by using simulated water table records to test the methodology. This methodology was also applied to a sample data set, and comparison with potential *ET* rates suggests that the results are realistic. While the general ET_G patterns can be extracted from the record, there are three sources of error that should be considered. First, even though random error was added to the simulation data here, and the field data contains noise, both of these cases have a very good signal to noise ratio. This is partially because the magnitude of the fluctuation is relatively large due to the moderate to high rates of ET_G combined with low values of readily available specific yield. In cases where the ratio of signal to noise is not as favorable, it may be necessary to fit the slope to five (or even more), data points rather than only three. Second, when the direction or rate of water table rise/fall is changing quickly, the value of the readily available specific yield is not constant and will introduce corresponding, transient error. Third, uncertainty associated with estimating the readily available specific yield translates directly to error in the estimate of ET_G.

For this analysis, the period from midnight to 6am was selected for the recovery analysis. However, the choice of this time period is somewhat subjective, and a slightly different period may be better at other sites. The optimal period for analysis may even shift and change in duration throughout the growing season. In general, it is preferable to have the longest possible period for determination of $\Gamma(WT_{DT})$. However, if the plant has the ability to store a significant volume of water, and the water status of the plant has been depleted during the day, uptake of water by the plant roots may continue for several

311 hours after the plant has stopped transpiring for the day in order to replenish the water
312 status of the plant. For this reason, the hours immediately after sunset should not be used
313 in determination of $\Gamma(WT_{DT})$. In addition, if hydraulic redistribution is a significant
314 process, root water uptake from the saturated zone may never be zero, and an assumption
315 of this analysis will be violated.

316 Well construction and well placement must be carefully considered to obtain
317 reasonable results with the proposed methodology. Wells must be screened across the
318 watertable and should be of small diameter to ensure that watertable fluctuations can be
319 adequately monitored and are not impacted by well bore storage effects that are
320 associated with large wells. In addition, watertable fluctuations are a result of root water
321 uptake not at the point location of the well, but rather as result of root water uptake over
322 some region. This region is the support scale of the measurement and is a function the
323 hydraulic properties of the sediment and the rate of water consumption (Loheide et. al
324 2005 and Jin et al, 2007). Wells should not be placed near streams, ponds, or vegetation
325 boundaries to avoid obtaining erroneous ET_G estimates.

326 In the development of the theory presented here, two cases were considered. The
327 first was the unlikely case of a source of water with a constant head in the vicinity of the
328 observation well. Driven by the difference in hydraulic head caused by vegetative
329 extraction of water near the water table, groundwater flow would occur from this source
330 toward the observation well. As the water table drops, the recovery rate would continue
331 to get stronger and stronger each day as a steeper groundwater gradient develops. We
332 also propose a second, more likely case, in which it is assumed that the water table and
333 the head at the recovery source both drop at a very similar rate; however, the head at the

334 source is always higher and does not exhibit diurnal fluctuations (Figure 1). The
335 appropriateness of this assumption can be evaluated by overlaying plots of dWT_{DT}/dt *vs*
336 WT_{DT} for the night preceding and following the day of interest (see Figure 4d and Figure
337 5). If the data from these two periods form a single, unique relationship, the assumption
338 is reasonable and detrended water depth can be used to estimate dWT_{DT}/dt *vs* WT_{DT}. This
339 second case was the one generally found in both the synthetic and field examples. While
340 an intermediate case is not considered in this analysis, there is a third case that should be
341 mentioned: the head at the recovery source is neither constant nor changing at a rate
342 similar to the trend of the water table. This case can be identified when neither the
343 dWT_{DT}/dt vs. WT (Figure 4c) nor the dWT_{DT}/dt vs. WT_{DT} (Figure 4d) result in a single
344 relationship for both the night before and after the period of interest. Significant changes
345 in the rate of ET_G from one day to the next can cause this third case to occur. Though the
346 relationships, $\Gamma(WTDT)$, before and after the time of interest are only slightly different
347 for day 7 as shown in Figure 5, this indicates that this situation may be realistic under
348 some conditions. This is the most general case and can theoretically be dealt with by
349 removing a slope other than the observed trend from the observed record. In equation 4,
350 we have chosen to remove a trend slope from the water table for the period of anlysis,
351 though this equation is valid for any arbitrary slope as well. In the general case, the slope
352 could be adjusted as necessary to collapse the depth versus recovery curves from the
353 morning of and the morning after the day of interest onto one another. The partial
354 detrending coefficients would have to be identified such that partial detrending resulted in
355 a single, well defined function, $\Gamma(WT_{DT})$. A full investigation of this case is beyond the
356 scope of this work.

357 The impetus for this research came from the recent results reported by Schilling
358 [2007] and Schilling and Kiniry [2007]. Both articles present hourly water table
359 fluctuations that show diurnal water table fluctuations that have a stepped pattern where
360 ET causes the water table to fall during the day and then the water table remains
361 relatively flat during the night for their sites, which are vegetated with reed canary grass
362 and corn. Because the recovery rate is nearly zero at these sites, the authors are able to
363 multiply the hourly water table difference by the specific yield to obtain an hourly plant
364 water use rate. However, a survey of data reported in the literature including the riparian
365 forest site investigated by Schilling [2007] and many others (e.g., [White, 1932; Troxell,
366 1936; Gatewood et al., 1950; Meyboom, 1967; Loheide et al., 2005; Butler et al., 2007;
367 Lautz, 2007]), demonstrate that this stepped pattern is not the typical case. There was
368 therefore a need to generalize the methodology of Schilling [2007] and Schilling and
369 Kiniry [2007]. When there is a non-zero recovery rate, this flux must be estimated and
370 accounted for to estimate hourly, or subhourly, ET_G. The method presented here provides
371 a means to accomplish this even when the recovery rate is not constant. This new
372 technique provides a relatively inexpensive means of estimating ET_G over extended
373 periods of time from areas with a shallow water table.
374
375 **Acknowledgments**
376 Financial support of this work was provided by the Wisconsin Alumni Research
377 Foundation. The sample data set was collected under grant EAR-0337393 provided by
378 the National Science Foundation. Any opinions, findings, and conclusions or
379 recommendations expressed in this material are mine and do not necessarily reflect the

380 views of the Wisconsin Alumni Research Foundation or the National Science
381 Foundation. I would also like to thank Eric Booth, Jessica Lundquist, James Butler, and
382 two anonymous reviewers for helpful discussions and comments on an earlier version of
383 this manuscript.
384

References:

Allen RG, Pereira LS, Raes D, Smith M. 1998, Crop Evapotranspiration - Guidelines for computing crop water requirements, *FAO Irrig. Drain. Pap.,* **56**, 300 pp.

Bleby, TM, Aucote M, Kennett-Smith AK, Walker GR, and Schachtman DP. 1997. Seasonal water use characteristics of tall wheatgrass [Agropyron elongatum (Host) Beauv.] in a saline environment, *Plant Cell Environ*., **20**, 1361– 1371.

Bond, BL, Jones JA, Moore G, Phillips N, Post D, and McDonnell JJ. 2002. The zone of vegetation influence on baseflow revealed by diel patterns of streamflow and vegetation water use in a headwater basin, *Hydrol. Processes*, **16**, 1671– 1677.

Butler JJ, Kluitenberg GJ, Whittemore DO, Loheide SP, Jin W, Billinger MA, and Zhan X. 2007. A field investigation of phreatophyte-induced fluctuations in the water table, *Water Resources Research* **43.** W02404. doi:10.1029/2005WR004627.

Cardenas, M. B., and J. L. Wilson, Exchange across a sediment-water interface with ambient groundwater discharge, *Journal of Hydrology*, **346**, 3-4, doi:10.1016/j.jhydrol.2007.08.019, 69-80, 2007.

Constantz, J. 1998. Interaction between stream temperature, streamflow, and groundwater exchanges in alpine streams, *Water Resour. Res.,* 34(7), 1609– 1615 doi:10.1029/98WR00998.

Czikowsky, MJ, Fitzjarrald DR. 2004. Evidence of Seasonal Changes in Evapotranspiration in Eastern U.S. Hydrological Records. *J. Hydrometeorology*. **5**: 974-988, 2004.

Eamus D., Froend L. 2006. Groundwater-dependent ecosystems: The where, what and why of GDEs. *Australian Journal of Botany* **54**, no. 2: 91–96.

Engel V, Jobbágy EG, Stieglitz M, Williams M, Jackson RB. 2005. Hydrological consequences of Eucalyptus afforestation in the Argentine Pampas. *Water Resources Research*, **41**:W10409. doi:10.1029/2004WR003761.

Gatewood JS, Robinson TW, Colby BR, Hem JC, Halpenny LC. 1950. Use of water by bottom-land vegetation in lower Safford Valley, Arizona, *U.S. Geol. Surv. Water Supply Pap., 1103.*

Jin W, Kluitenberg GJ, Butler JJ. 2007. Analytical Solutions for Examining Spatial Variations in Evapotranspiration-Driven Fluctuations in the Water Table in Vegetated Riparian Zones. *Eos Trans. AGU*, **88**(52), Fall Meet. Suppl., Abstract H13B-1246.

Lautz LK. 2007. Estimating groundwater evapotranspiration rates using diurnal water table fluctuations in a semi-arid riparian zone, *Hydrogeology Journal* doi 10.1007/s10040-007-0239-0

Loheide SP, Gorelick SM. 2007. Riparian hydroecology: A coupled model of the observed interactions between groundwater flow and meadow vegetation patterning, *Water Resources Research* **43.** W07414. doi:10.1029/2006WR005233.

Loheide SP, Gorelick SM. 2006. Quantifying stream-aquifer interactions through analysis of remotely sensed thermographic profiles and in-situ temperature records, *Environmental Science & Technology* **40**: 3336-3341. doi:10.1021/es0522074.

Loheide SP, Gorelick SM. 2005. A high-resolution evapotranspiration mapping algorithm (ETMA) with hydroecological applications at riparian restoration sites, *Remote Sensing of Environment* **98**: 182-200. doi:10.1016/j.rse.2005.07.003.

Loheide SP, Butler JJ, Gorelick SM. 2005. Estimation of groundwater consumption by phreatophytes using diurnal water table fluctuations: A saturated-unsaturated flow assessment, *Water Resources Research* **41**, W07030, doi:10.1029/2005WR003942.

Lundquist J., Cayan D. 2002. Seasonal and spatial patterns in diurnal cycles in streamflow in the Western United States. *J. Hydromet*., **3**, 591-603

Meyboom P. 1967. Groundwater studies in the Assiniboine River drainage basin—part II: Hydrologic characteristics of phreatophytic vegetation in south-central Saskatchewan, *Bull. Geol. Surv. Can. ,139.*

Nachabe MH. 2002. Analytical expressions for transient specific yield and shallow water table drainage, *Water Resources Research* **38**:10 1193, doi:10.1029/2001WR001071.

Schilling KE. 2007. Water table fluctuations under three riparian land covers, Iowa (USA), *Hydrological Processes*, doi:10.1002/hyp6393.

Schilling KE, Kiniry JR. 2007. Effects of land cover on water table, soil moisture, evapotranspiration, and groundwater recharge: A Field observation and analysis *Journal of Hydrology,* **337**: 356–363. doi:10.1016/j.jhydrol.2007.02.003

Troxell HC. 1936. The diurnal fluctuation in the ground-water and flow of the Santa Ana river and its meaning, *Eos Trans*. AGU, **17(4):** 496–504.

van Genuchten M. 1980. A closed-form equation for predicting the hydraulic conductivity of unsaturated soils, *Soil Sci. Soc. Am. J.,* **44**: 892–898.

White WN. 1932. A method of estimating ground-water supplies based on discharge by plants and evaporation from soil: Results of investigations in Escalante Valley, Utah, *U.S. Geol. Surv. Water Supply Pap*., 659-A.

474

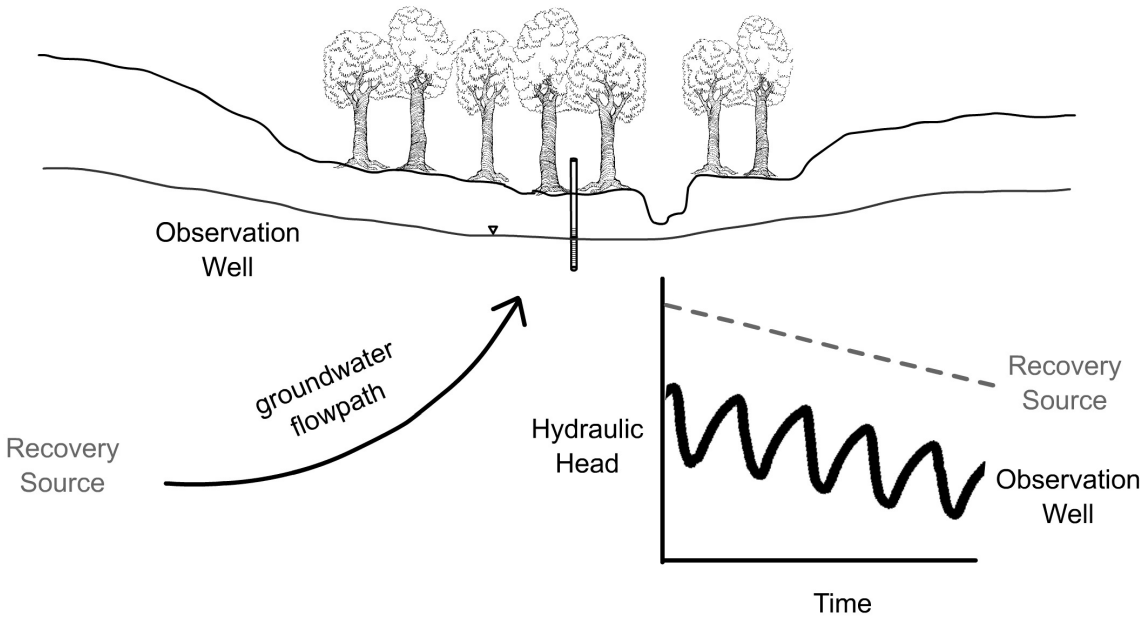

475

476 Figure 1 – Conceptual diagram showing groundwater flow toward a riparian area where it
477 discharges via root uptake by phreatophytic vegetation. Observation wells screened
478 across the water table in this environment typically show diel, ET_G induced fluctuations.
479 While these fluctuations exist at the water table in the riparian zone, they are muted at
480 distances up-gradient along the groundwater flowpath.

481

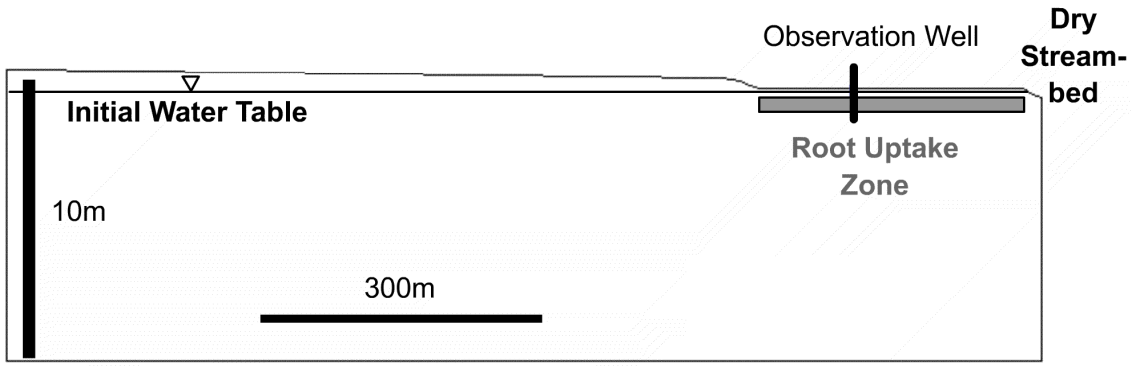

482

483 Figure 2 – Simulation flow domain showing location of root water uptake zone and

484 observation location.

485

486

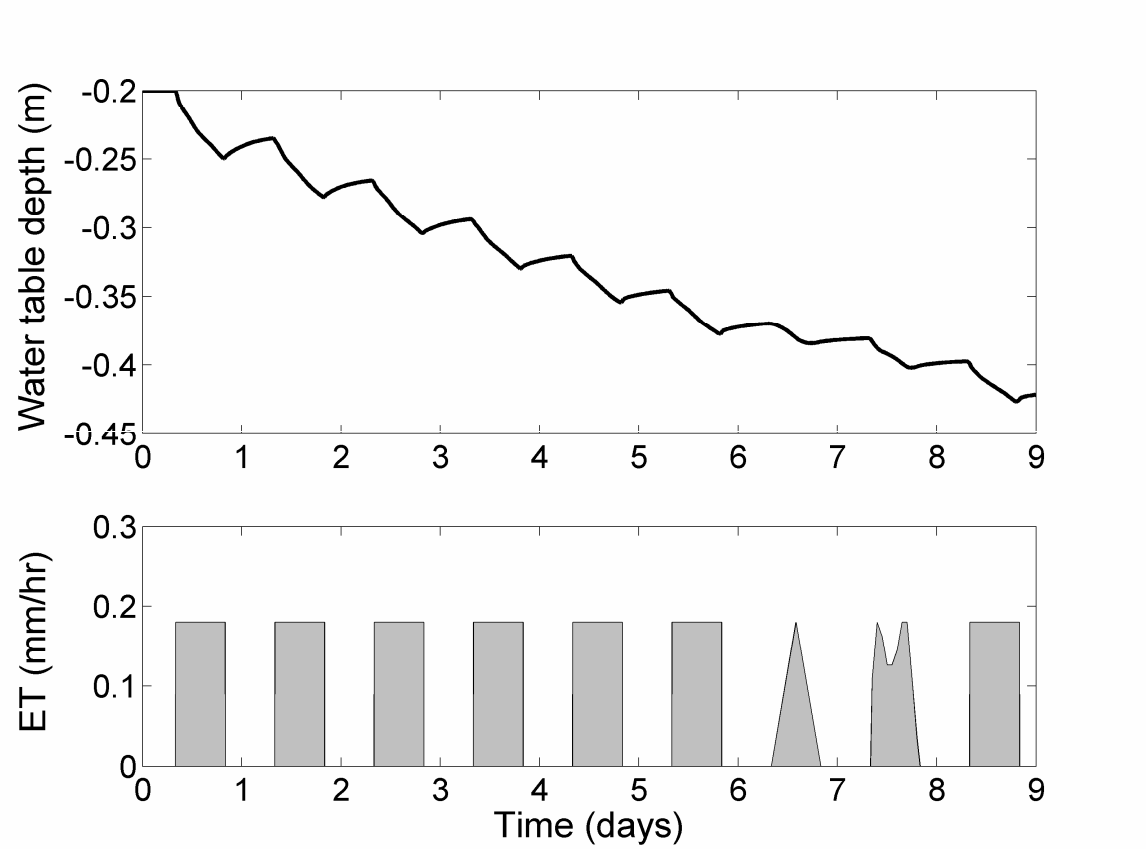

487

488 Figure 3 – [Top] Simulated water table fluctuations [Bottom] Temporal pattern of root

489 water uptake.

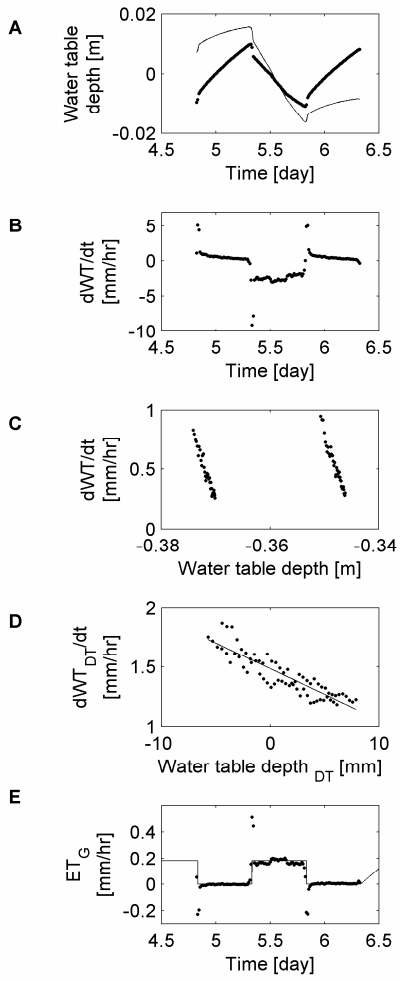

Figure 4 – Intermediate results demonstrating the data processing method proposed here. A) Raw (vertically shifted, thin line) and detrended (thick line) water table fluctuation from the period from 8pm on the day prior to the day of interest to 8am on the day after the day of interest B) Time rate of change of the water table elevation as it changes with time C) Time rate of change of the water table elevation as it changes with water table depth; the data show two separate linear relationships for each period of zero ET_G D) Time rate of change of the detrended water table elevation as it changes with detrended water table depth; the two curves shown in C collapse to form a single relationship as a function of detrended water table depth E) Estimated ET_G for this time period (circles) and input ET_G (line)

501

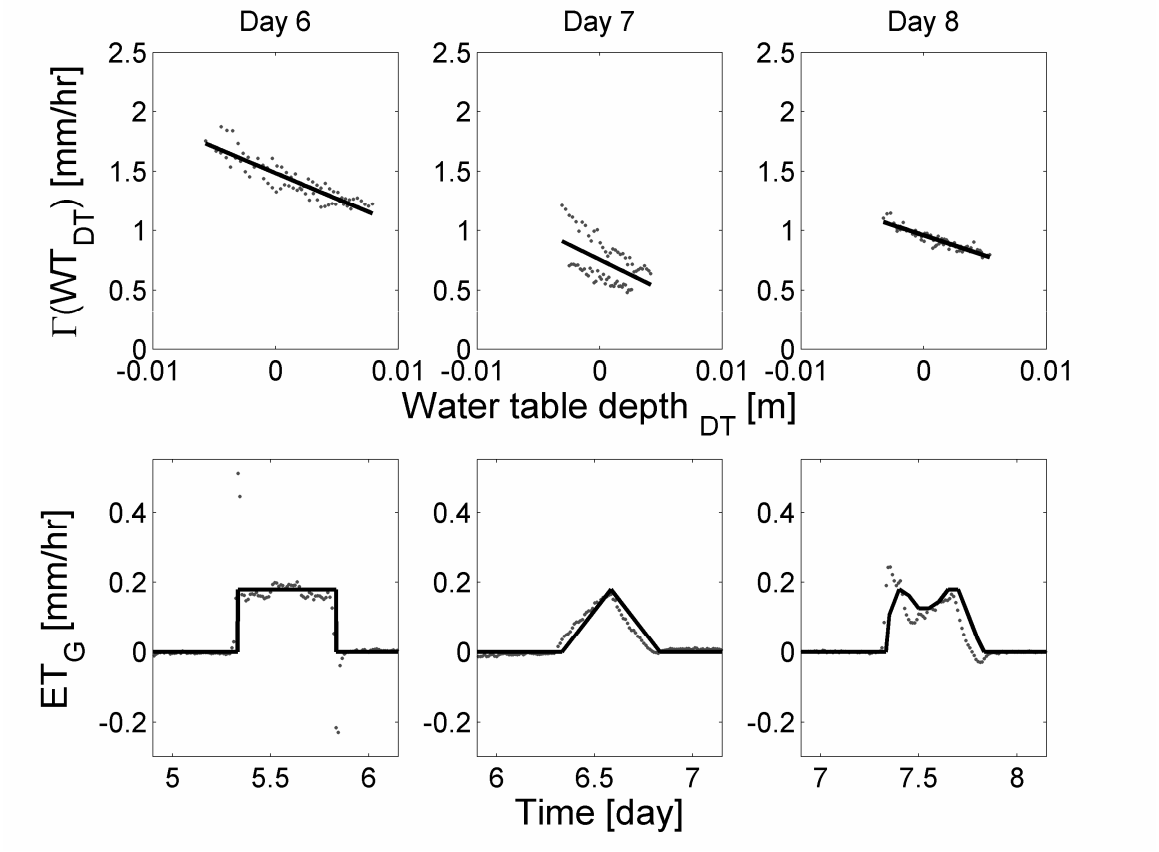

502

503 Figure 5 - The relationship between the time rate of change of the detrended water table

504 position and the detrended water table depth with the best-fit estimate of $\Gamma(WT_{DT})$ [top

505 row] and the estimated (points) and actual (line) ET_G [bottom row] is shown for the

506 square wave (day 6), triangular (day 7), and double-peaked (day 8) patterns of ET_G.

507

508

509

510

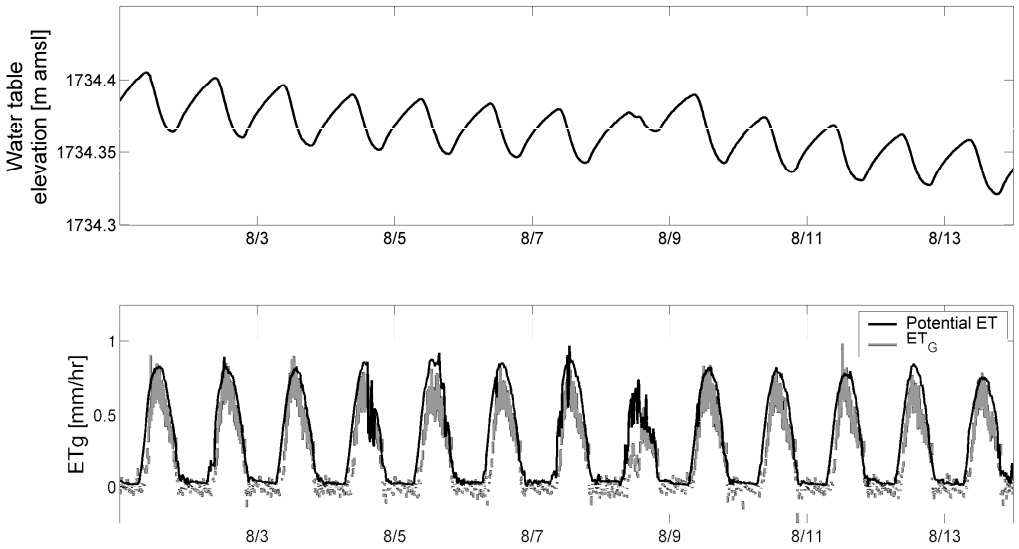

511

512 Figure 6- [Top] Water table fluctuations recorded in riparian meadow supporting

513 phreatophytic sedges. [Bottom] Estimated ET_G from the water table record and potential

514 *ET*.

515

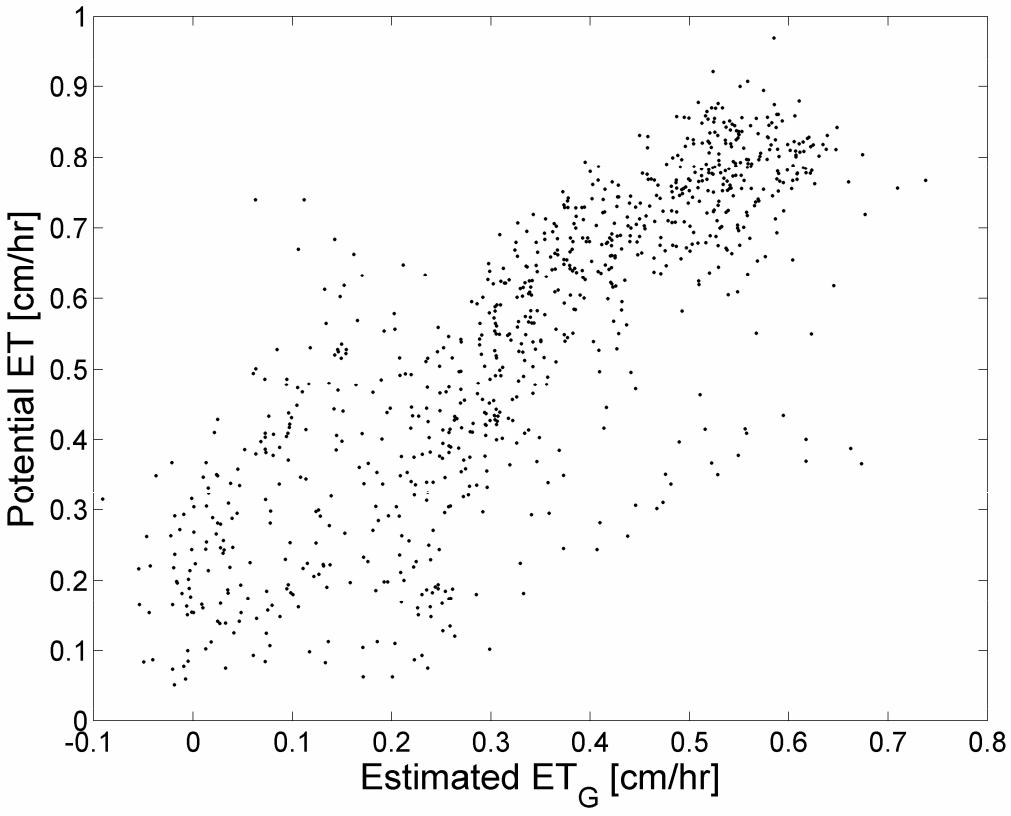

516

517 Figure 7- Potential ET has been plotted against estimated ET_G using a S_y^*=0.08. Since

518 the plot is comparing potential ET with the groundwater component of actual ET, a 1:1

519 relationship is not expected; however a correlation between these parameters is

520 demonstrated.